



**HAL**  
open science

# Use of integral data assimilation and differential measurements as a contribution to improve $^{235}\text{U}$ and $^{235}\text{U}$ cross sections evaluations in the fast and epithermal energy range

Virginie Huy, Gilles Noguere, G. Rimpault

## ► To cite this version:

Virginie Huy, Gilles Noguere, G. Rimpault. Use of integral data assimilation and differential measurements as a contribution to improve  $^{235}\text{U}$  and  $^{235}\text{U}$  cross sections evaluations in the fast and epithermal energy range. EPJ N - Nuclear Sciences & Technologies, 2018, 4, pp.41. 10.1051/epjn/2018035 . cea-02305677

HAL Id: cea-02305677

<https://cea.hal.science/cea-02305677>

Submitted on 4 Oct 2019

**HAL** is a multi-disciplinary open access archive for the deposit and dissemination of scientific research documents, whether they are published or not. The documents may come from teaching and research institutions in France or abroad, or from public or private research centers.

L'archive ouverte pluridisciplinaire **HAL**, est destinée au dépôt et à la diffusion de documents scientifiques de niveau recherche, publiés ou non, émanant des établissements d'enseignement et de recherche français ou étrangers, des laboratoires publics ou privés.



Distributed under a Creative Commons Attribution 4.0 International License

# Use of integral data assimilation and differential measurements as a contribution to improve $^{235}\text{U}$ and $^{238}\text{U}$ cross sections evaluations in the fast and epithermal energy range

Virginie Huy<sup>1,2,\*</sup>, Gilles Noguère<sup>1</sup>, and Gérald Rimpault<sup>1</sup>

<sup>1</sup> CEA, DEN, DER, SPRC Cadarache, 13108 St Paul-Lez-Durance, France

<sup>2</sup> ED352 Doctoral School, AMU, Luminy Campus, 13288 Marseille, France

Received: 7 December 2017 / Received in final form: 1 March 2018 / Accepted: 22 May 2018

**Abstract.** Critical mass calculations of various HEU-fueled fast reactors result in large discrepancies in C/E values, depending on the nuclear data library used and the configuration modeled. Thus, it seems relevant to use integral experiments to try to reassess cross sections that might be responsible for such a dispersion in critical mass results. This work makes use of the Generalized Least Square method to solve Bayes equation, as implemented in the CONRAD code. Experimental database used includes ICSBEP Uranium based critical experiments and benefits from recent re-analyses of MASURCA and FCA-IX criticality experiments (with Monte-Carlo calculations) and of PROFIL irradiation experiments. These last ones provide very specific information on  $^{235}\text{U}$  and  $^{238}\text{U}$  capture cross sections. Due to high experimental uncertainties associated to fission spectra, we chose to consider either fitting these data or set them to JEFF-3.1.1 evaluations. The work focused on JEFF-3.1.1  $^{235}\text{U}$  and  $^{238}\text{U}$  evaluations and results presented in this paper for  $^{235}\text{U}$  capture and  $^{238}\text{U}$  capture, and inelastic cross sections are compared to recent differential experiment or recent evaluations. Our integral experiment assimilation work notably suggests a 30% decrease for  $^{235}\text{U}$  capture around 1–2.25 keV, a 10% increase in the unresolved resonance range when using JEFF-3.1.1 as “a priori” data. These results are in agreement with recent microscopic measurements from Danon et al. [Nucl. Sci. Eng. **187**, 291 (2017)] and Jandel et al. [Phys. Rev. Lett. **109**, 202506 (2012)]. For  $^{238}\text{U}$  cross sections, results are highly dependent on fission spectra.

## 1 Introduction

Critical mass calculations of various HEU-fueled fast reactors result in large discrepancies in C/E values, depending on flux spectra, fuel enrichment, structural materials present and so on. These C/E values, calculated with the Monte-Carlo code TRIPOLI-4 [1], are shown in Figure 1. Table 1 gives some specifications about fuel and structural materials present in each configuration.

Figure 1 underlines that critical mass C/E values for Uranium-fueled configurations of Fast Reactors calculated with JEFF-3.2 library are systematically overestimated (except for BIGTEN and GODIVA) and are larger than those calculated with JEFF-3.1.1. Discrepancy between the two sets of calculations goes from ~250 to ~630 pcm for BIGTEN. Moreover, large C/E values are observed for FCA-IX configurations (overestimation up to ~800 pcm), BIGTEN and GODIVA when using the JEFF-3.1.1 library. Except for FLATTOP- $^{235}\text{U}$ , all critical masses for configurations with HEU fuel exceed experimental uncertainties

when using JEFF-3.1.1. Although MASURCA 1B and FCA-IX configurations [2] have similar spectra (as they both contain graphite) but significantly different Uranium enrichments and geometries, the large discrepancy observed in their C/E values (using either JEFF-3.1.1 or JEFF-3.2) rise concerns of possible compensating errors between  $^{235}\text{U}$  and  $^{238}\text{U}$  evaluations in the JEFF libraries in the fast and epithermal energy range.

## 2 Integral experiments assimilation

Considering the very large C/E values presented in Section 1, it seems relevant to use integral data assimilation to identify which nuclear data are responsible for these discrepancies. This was performed using the CONRAD code from CEA [3], which can solve analytically Bayes' theorem.

### 2.1 Bayesian inference

As a reminder, Bayes' theorem [4] generalized to continuous probability densities is given:

\* e-mail: [virginie.huy@cea.fr](mailto:virginie.huy@cea.fr)

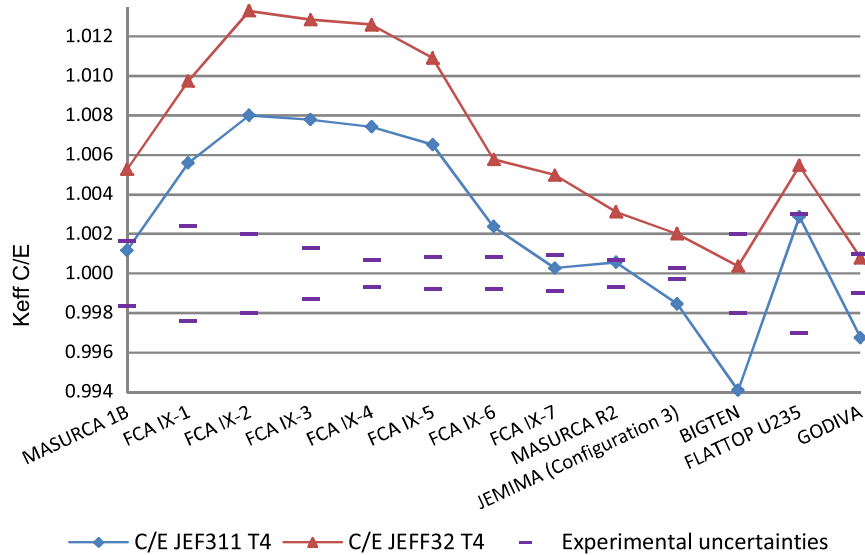


Fig. 1. Critical mass C/Es compared with experimental uncertainties for Uranium configurations (using JEFF libraries).

Table 1. Specifications on fuel enrichment and structural materials for the different configurations.

Configuration	Fuel enrichment	Structural material and diluents
FCA-IX 1	93% (with Udep blanket)	Graphite
FCA-IX 2	93% (with Udep blanket)	Graphite
FCA-IX 3	93% (with Udep blanket)	Graphite
FCA-IX 4	93% (with Udep blanket)	Stainless steel
FCA-IX 5	93% (with Udep blanket)	Stainless steel
FCA-IX 6	93% (with Udep blanket)	Stainless steel
FCA-IX 7	20% (with Udep blanket)	–
MASURCA 1B	30% (with Unat blanket)	Graphite
MASURCA R2	30% (with Unat blanket)	Sodium
JEMIMA (configuration 3)	Alternation of HEU (93.4%) fuel and Unat disks	Steel
BIGTEN	10% in average (with Udep reflector)	Steel
FLATTOP- <sup>235</sup> U	93% (with Unat reflector)	–
GODIVA	94%	–

$$\underbrace{p(\mathbf{x}|\mathbf{y},U)}_{\text{posterior}} = \frac{p(\mathbf{y}|\mathbf{x},U) \cdot p(\mathbf{x},U)}{\int p(\mathbf{y}|\mathbf{x},U) \cdot p(\mathbf{x},U) \cdot d\mathbf{x}} \propto \underbrace{p(\mathbf{y}|\mathbf{x},U)}_{\text{likelihood}} \underbrace{p(\mathbf{x},U)}_{\text{prior}}, \quad (1)$$

where the vector  $\mathbf{x}$  contains the parameters to be reassessed (in our case, the 33-group cross sections) in the view of new observations enclosed in the vector  $\mathbf{y}$ .  $U$  gathers all the “background” information, that is, hypotheses or approximations made to obtain the values for  $\mathbf{x}$  and  $\mathbf{y}$ .

In practice, probability densities associated to each multigroup cross-section are assumed to be Gaussian distributions, as this choice maximizes the entropy [5]. Using Laplace approximation [6], we then assume that the posterior probability density function solution of equation (1) can be well-approximated by a Gaussian distribution:

$$p(\sigma|\mathbf{E} - \mathbf{C}(\sigma), U) \propto e^{-\frac{1}{2}((\sigma - \sigma_{\text{priori}})^T M_{\sigma}^{-1} (\sigma - \sigma_{\text{priori}}) + (\mathbf{E} - \mathbf{C}(\sigma))^T M_{\mathbf{E}}^{-1} (\mathbf{E} - \mathbf{C}(\sigma)))}, \quad (2)$$

where  $\mathbf{E}$  is a vector containing integral measurements values,  $\mathbf{C}$  is a vector containing associated calculated values,  $M_{\sigma}$  is the covariance matrix associated to nuclear data  $\sigma$ ,  $M_{\mathbf{E}}$  is the covariance matrix associated to C/E values.

For a Gaussian distribution, the central value is associated to its maximum. Thus, optimal solutions for  $\sigma$  and associated covariances,  $M_{\sigma}$  are determined by minimizing a cost function (using Generalized Least Square method):

**Table 2.** Experimental correlation matrix for PROFIL-2A C/E.

		E1		E8		E21		E28	E35		E42	
		<sup>8</sup> U	<sup>5</sup> U	<sup>8</sup> U	<sup>5</sup> U	<sup>8</sup> U	<sup>5</sup> U	<sup>5</sup> U	<sup>8</sup> U	<sup>5</sup> U	<sup>8</sup> U	<sup>5</sup> U
E1	<sup>8</sup> U	1.00	0.92	0.86	0.92	0.86	0.92	0.92	0.85	0.92	0.85	0.92
	<sup>5</sup> U	0.92	1.00	0.92	0.99	0.92	0.99	0.99	0.92	0.99	0.91	0.99
E8	<sup>8</sup> U	0.86	0.92	1.00	0.92	0.86	0.92	0.92	0.86	0.92	0.85	0.92
	<sup>5</sup> U	0.92	0.99	0.92	1.00	0.92	0.99	0.99	0.92	0.99	0.91	0.99
E21	<sup>8</sup> U	0.86	0.92	0.86	0.92	1.00	0.92	0.92	0.86	0.92	0.85	0.92
	<sup>5</sup> U	0.92	0.99	0.92	0.99	0.92	1.00	0.99	0.92	0.99	0.91	0.99
E28	<sup>5</sup> U	0.92	0.99	0.92	0.99	0.92	0.99	1.00	0.92	0.99	0.91	0.99
E35	<sup>8</sup> U	0.85	0.92	0.86	0.92	0.86	0.92	0.92	1.00	0.92	0.85	0.92
	<sup>5</sup> U	0.92	0.99	0.92	0.99	0.92	0.99	0.99	0.92	1.00	0.91	0.99
E42	<sup>8</sup> U	0.85	0.91	0.85	0.91	0.85	0.91	0.91	0.85	0.91	1.00	0.91
	<sup>5</sup> U	0.92	0.99	0.92	0.99	0.92	0.99	0.99	0.92	0.99	0.91	1.00

$$\chi_{GLS}^2 = (\sigma - \sigma_{\text{a priori}})^T M_{\sigma}^{-1} (\sigma - \sigma_{\text{a priori}}) + (\mathbf{E} - \mathbf{C}(\sigma))^T M_{\mathbf{E}}^{-1} (\mathbf{E} - \mathbf{C}(\sigma)). \quad (3)$$

## 2.2 Integral data assimilation strategy and results for posterior C/E

The JEFF-3.1.1 library was chosen as the a priori as it gives more satisfying results than JEFF-3.2 for Uranium configurations sensitive to the fast energy range, as seen in Figure 1. For our assimilation work, we used critical mass C/E of MASURCA 1B, FCA-IX cores 1–7, FLATTOP-<sup>235</sup>U and GODIVA, as well as variations of concentration ratios C/E from PROFIL-2A irradiation experiments [7,8]. Experimental correlation matrix for FCA-IX configurations is provided in reference [2]. Experimental correlation matrix for PROFIL experiments is given in Table 2. In this table, “<sup>8</sup>U” refers to the ratio variation  $\Delta \frac{^{235}\text{U} + ^{238}\text{U}}{^{238}\text{U}}$  and “<sup>5</sup>U” refers to the ratio variation  $\Delta \frac{^{236}\text{U}}{^{235}\text{U}}$ .

C/E used in the assimilation work were calculated using the Monte-Carlo code TRIPOLI-4 (except for PROFIL’s variation of concentrations ratios, calculated with ECCO/ERANOS) and 33-group sensitivity coefficients to nuclear data were calculated using the ECCO/ERANOS code [9]. For nuclear data covariance matrices, we used COMACV1.0 [10], except for <sup>235</sup>U  $\nu$  for which we used the COMMARA-2.0 matrix [11].

Critical mass C/E values for these configurations provide a great variety of sensitivity profiles to <sup>235</sup>U capture and <sup>238</sup>U capture and inelastic cross sections (this is shown for <sup>235</sup>U capture in Fig. 2). Using all these C/E values with their associated sensitivity coefficients in a single assimilation calculation allows us to make the most of both the redundant or complementary information they provide for the whole fast energy range.

Notably, the simultaneous use of GODIVA and FLATTOP-<sup>235</sup>U critical masses can help avoiding compensations between <sup>235</sup>U and <sup>238</sup>U cross sections, as these fast spectrum critical configurations are similar, except for the presence of natural Uranium reflector in

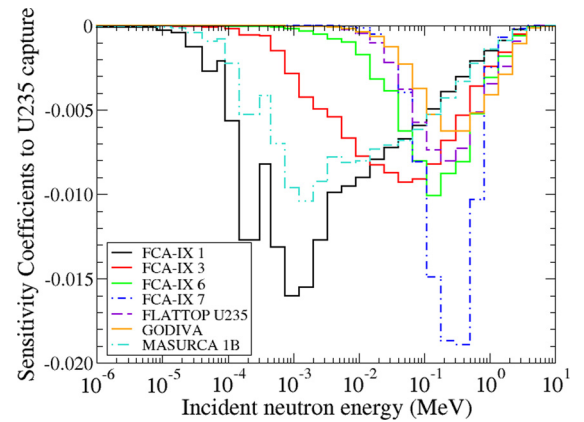


**Fig. 2.** 33-group sensitivity profiles of several critical masses to <sup>235</sup>U capture.

FLATTOP-<sup>235</sup>U. Critical mass sensitivities to <sup>238</sup>U inelastic and capture and <sup>235</sup>U capture cross sections for these two configurations are shown in Figure 3. One can see that critical mass sensitivities to <sup>235</sup>U cross sections are similar whereas sensitivity coefficients to <sup>238</sup>U cross sections are important for FLATTOP-<sup>235</sup>U and low for GODIVA.

The nuclear data fitted through assimilation are <sup>235</sup>U and <sup>238</sup>U capture, elastic, inelastic 33-groups cross sections as well as their fission spectrum  $\chi$  (unless specified otherwise) and multiplicity  $\nu$ . <sup>235</sup>U and <sup>238</sup>U fission were not fitted, as JEFF-3.1.1 evaluations are in good agreement with Neutron Standard from IAEA [12] for these cross sections. Also, it should be noted that assimilation work does not take into account sensitivities to angular distributions as no covariance matrices are currently available for these data. Taking into account these approximations through marginalization is the topic of future works.

In this integral data assimilation work, an effort was made to try to reduce risks of compensating errors by relying on the Neutron Cross-section Standards [12] for <sup>235</sup>U and <sup>238</sup>U fission cross sections and by using PROFIL-2A C/E (which add a specific constraint on <sup>235</sup>U or <sup>238</sup>U capture cross sections).

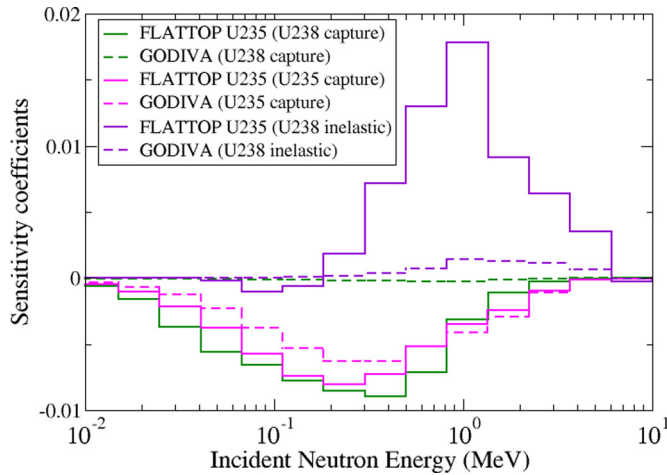


**Fig. 3.** Sensitivity coefficients of FLATTOP- $^{235}\text{U}$  and GODIVA critical masses to  $^{235}\text{U}$  capture and  $^{238}\text{U}$  inelastic and capture cross sections.

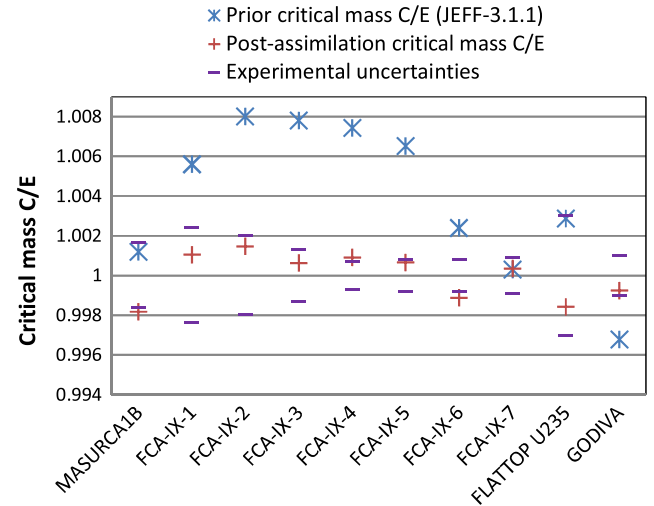


**Fig. 4.** Comparison between prior (JEFF-3.1.1) and posterior C/E values.

**Table 3.** Impact on MASURCA 1B and FCA-IX 1 to 3 critical masses when using carbon evaluation of JENDL-4.0 instead of JEFF-3.1.1.

	MASURCA 1B	FCA-IX-1	FCA-IX-2	FCA-IX-3
Impact on critical mass	-260 pcm	-420 pcm	-280 pcm	-230 pcm

Nevertheless, as this will be shown in the following sections, high uncertainties associated to fission spectra can have a significant impact on assimilation result. Also, as differences in JEFF-3.1.1 and JENDL-4.0 carbon evaluations were found to have a non-negligible impact for some critical masses used in this work (Tab. 3), we ran CONRAD calculations for both of these options. For these reasons, the results presented in Section 3 are sets of trends that include the four alternatives considered: fission spectra fitted or not and carbon evaluation either from JEFF-3.1.1 or JENDL-4.0. Assimilation trends are presented in this manner to stress that the variability in the results due to these choices can be seen as additional uncertainties.

Experimental correlations between FCA-IX critical mass C/E were taken into account using the matrix provided by JAEA [2]. Also, correlations between PROFIL irradiation experiments were calculated. Figure 4 displays post-assimilation C/E for critical masses compared with prior JEFF-3.1.1 C/E values for the case where fission spectra are set to JEFF-3.1.1 and JEFF-3.1.1 graphite evaluation is used. A priori and a posteriori C/E values for the PROFIL irradiation experiment are given in Table 4, along with experimental uncertainties.

Post-assimilation C/E values are well-included in  $1\sigma$  experimental uncertainties, except for MASURCA 1B and FCA-IX 6, which however remain in  $2\sigma$  total uncertainties. This means there exists an optimal set of cross sections for the experimental database taken into account, and no inconsistency between C/E had been found.

### 3 Comparison of assimilation trends with differential measurements

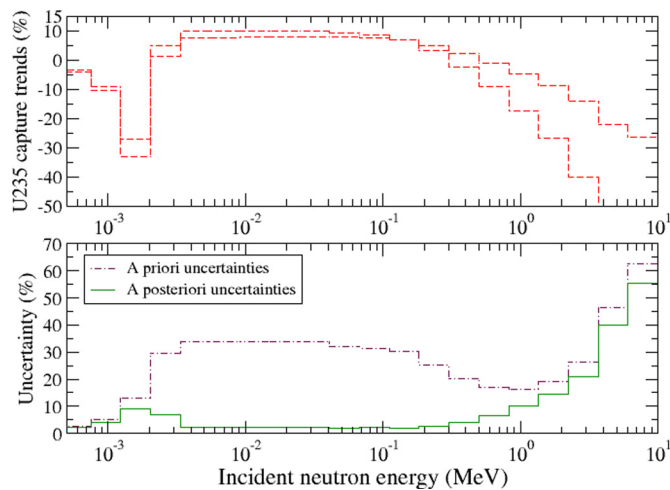
To discuss the reliability of the trends on cross sections suggested through the integral data assimilation, we compared them to recent differential measurements from the EXFOR database [13] when they are available or recent evaluations otherwise. In this section, trends are given relative to JEFF-3.1.1.

#### 3.1 $^{235}\text{U}$ capture cross section

Assimilation results suggest a significant modification for  $^{235}\text{U}$  capture: a  $\sim 30\%$  decrease around 1–2 keV and a  $\sim 10\%$  increase in the unresolved resonance range (URR) when using JEFF3.1.1 as “a priori” data. This is shown in Figure 5, along with prior and posterior uncertainties. One can notice that from 1 to 500 keV, posterior uncertainties are sufficiently low to consider assimilation trends as possible recommendations for a change in  $^{235}\text{U}$  capture cross section. As mentioned earlier, the two curves displayed in Figure 5 represent an envelope, in which the assimilation results for the following four cases are included: uncertainties on graphite evaluation choice (JEFF-3.1.1 or JENDL-4.0) and fission spectra (fitted or set to JEFF-3.1.1). For  $^{235}\text{U}$  capture cross sections, differences in posterior uncertainties for these four cases do not exceed 0.5% in the energy range of interest. Thus, only one curve is displayed in Figure 5.

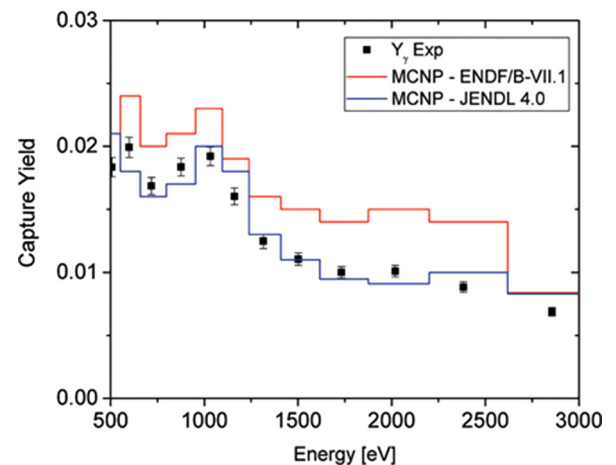
**Table 4.** Prior and posterior C/E values for PROFIL-2A variation of concentrations ratios and associated uncertainties.

C/E	Sample number	Prior C/E value	Posterior C/E value	Experimental and calculation
$\Delta \frac{U_{235}+U_{236}}{U_{238}}$	E1	0.999	1.004	1.3%
	E8	0.998	1.004	1.2%
	E21	0.997	1.003	1.2%
	E35	0.999	1.005	1.2%
	E42	0.999	1.005	1.2%
$\Delta \frac{U_{236}}{U_{235}}$	E1	1.004	1.015	1.6%
	E8	0.998	1.008	1.6%
	E21	0.996	1.006	1.6%
	E28	0.997	1.007	1.6%
	E35	0.997	1.006	1.6%
	E42	1.001	1.010	1.6%

**Fig. 5.** Trends from assimilation work for  $^{235}\text{U}$  capture (relative to JEFF-3.1.1) compared with a priori and a posteriori nuclear data uncertainties. The two red dotted curves represent an envelope gathering all the trends suggested by assimilation results (that includes cases with fission spectra fitted or not, and with graphite evaluation from JEFF-3.1.1 or JENDL-4.0).

Focusing on the end of the resolved resonances range (RRR) from 1 to 2.25 keV, we compared our assimilation trends in this energy range with recent differential measurements made at RPI. Figure 6 displays results of these measurements as published in reference [14] (as they are not currently available in the EXFOR database) with a comparison to ENDF/B-VII and JENDL-4.0. One has to note that for  $^{235}\text{U}$  capture cross section, JEFF-3.1.1 and ENDF/B-VII.1 evaluations are identical. This graph of Figure 6 shows that our assimilation results are in good agreement with Danon measurements at RPI as they suggest a  $\sim 33\%$  decrease of  $^{235}\text{U}$  capture cross section from JEFF-3.1.1 at around 2 keV. This issue on  $^{235}\text{U}$  capture was already addressed in WPEC Subgroup 29 [15], which underlined an overestimation of this cross section in the end of the RRR in the JEFF-3.1 evaluation.

In the URR, from 10 to 100 keV, most recent measurements performed by Jandel et al. [16] at LANSCE

**Fig. 6.** Results of differential measurements from Danon et al. [14] for  $^{235}\text{U}$  capture from 0.5 to 3 keV, compared with ENDF/B-VII.1 and JENDL-4.0 evaluations.

with the DANCE detector are consistent with assimilation trends from 3 keV to 1 MeV (Fig. 7).

Comparing now assimilation results to JEFF-3.3t3 [17] (in Fig. 8), one can see that they agree well in the end of the RRR (considering that assimilation results uncertainties in this range is around 9%). In the URR, from 10 to 100 keV, JEFF-3.3t3 evaluation suggests a higher increase from JEFF-3.1.1 (around 20%) than our assimilation results.

Figure 9 shows a comparison between Jandel et al. [16] measurements, JEFF-3.3t3 [17] and JEFF-3.1.1 evaluations. Compared to Jandel measurements, it seems that JEFF-3.3t3  $^{235}\text{U}$  capture cross section evaluation is slightly higher whereas JEFF-3.1.1 appears to underestimate this cross section in the 10–100 keV energy range.

### 3.2 $^{238}\text{U}$ capture cross section

Unlike  $^{235}\text{U}$  capture, trends for  $^{238}\text{U}$  capture are highly dependent on fission spectra values. As it can be seen in Figure 10, in the case where fission spectra are fitted through assimilation, resulting trends on  $^{238}\text{U}$  capture are included in posterior uncertainties. When fission spectra

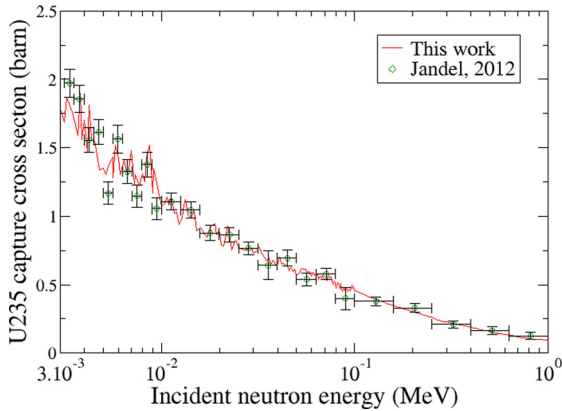


**Fig. 7.** Results of differential measurements from Jandel et al. [16] for  $^{235}\text{U}$  capture from 3 keV to 1 MeV. Comparison with assimilation results applied to JEFF-3.1.1 point-wise evaluations (red continuous line).

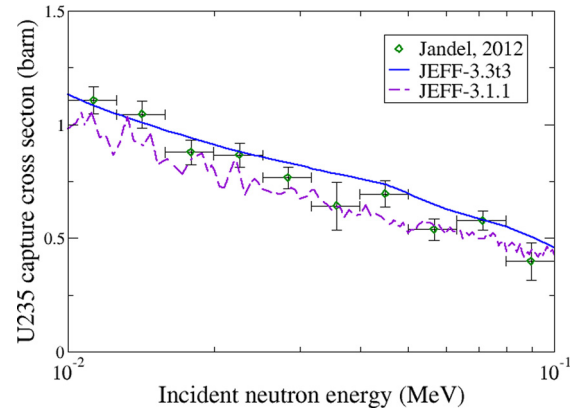


**Fig. 9.** Comparison of Jandel et al. measurements [16] to JEFF-3.3t3 and JEFF-3.1.1 evaluations for  $^{235}\text{U}$  capture cross sections.

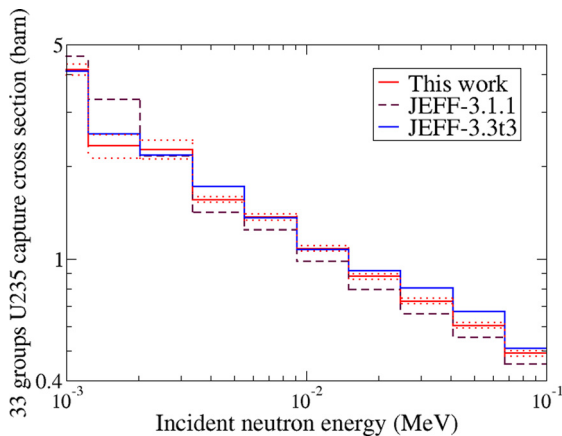


**Fig. 8.** 33-group assimilation results for  $^{235}\text{U}$  capture compared with “a priori” JEFF-3.1.1 and JEFF-3.3t3 evaluation. Posterior uncertainties for assimilation results are in dotted line.

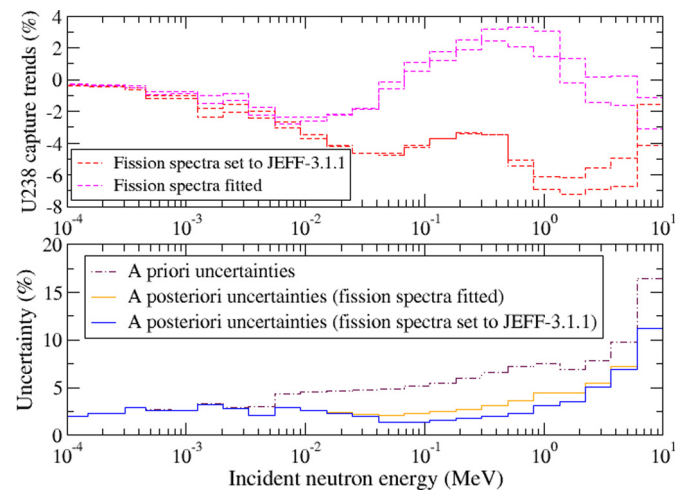


**Fig. 10.** Trends from assimilation work for  $^{238}\text{U}$  capture (relative to JEFF-3.1.1) compared with a priori and a posteriori nuclear data uncertainties. For both cases (fission spectra fitted or not), the two dotted lines have to be seen as an additional uncertainty associated to the choice of graphite evaluation.

are not fitted and set to JEFF-3.1.1, trends suggested ( $-4\%$  up to  $-7\%$  from JEFF-3.1.1) by the assimilation work are higher than posterior uncertainties from 10 keV to 3 MeV. Dependency of the results on fission spectra values is also reflected by the differences in posterior uncertainties for the two cases (Fig. 10). A posteriori uncertainties for  $^{238}\text{U}$  capture are noticeably higher in the case where fission spectra are fitted. However, one can notice that the choice for graphite evaluation has little impact on the results in both cases.

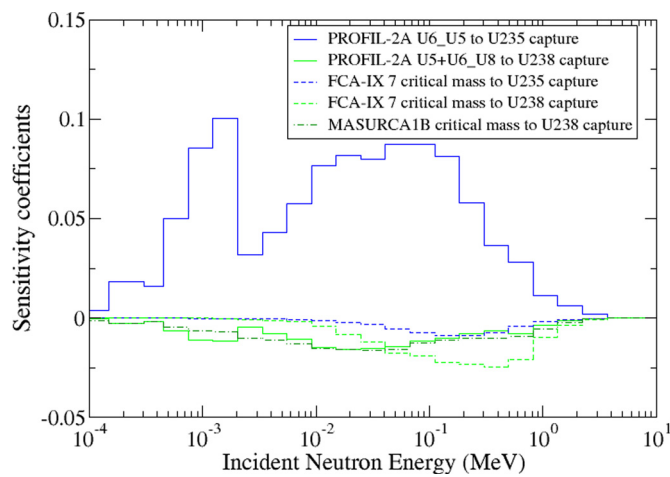
The dependency of assimilation results for  $^{238}\text{U}$  capture cross section can be explained by the fact that sensitivity coefficients of PROFIL ratio variations  $\Delta \frac{^{235}\text{U} + ^{236}\text{U}}{^{238}\text{U}}$  are at the same level as critical masses sensitivity coefficients for this cross section. Moreover, from 100 keV to 1 MeV, these sensitivity coefficients are noticeably lower than those of some critical masses. This is not the case for  $\Delta \frac{^{236}\text{U}}{^{235}\text{U}}$  whose sensitivity profile dominates all the critical mass sensitivity profiles to  $^{235}\text{U}$  capture. The constraint brought by PROFIL-2A C/E on  $^{238}\text{U}$  capture is thus less important

than for  $^{235}\text{U}$  capture. This is shown in Figure 11. Also, a priori correlations between  $^{238}\text{U}$  cross sections might amplify the impact of fission spectra on assimilation results.

In the end, the great impact of fission spectra on  $^{238}\text{U}$  capture results suggests possible compensations between  $^{238}\text{U}$  capture and  $^{238}\text{U}$  and  $^{235}\text{U}$  fission spectra in our assimilation work. This assimilation results for  $^{238}\text{U}$  capture cross section are all the more questioning as these can have a significant impact on fast reactor calculations. For instance, the trend suggested by the assimilation (for the case where fission spectra are set to JEFF-3.1.1) has an impact of around  $+500$  pcm on the reactivity of the SFR ASTRID. Details of this impact per energy group (for a 33-group sensitivity calculation) are given in Table 5. Thus, considering the high sensitivity of some fast reactors critical masses to this cross section, assimilation results should be clarified, for instance by using a wider experimental database for the assimilation.

**Table 5.** Relative impact on ASTRID critical mass of the trends suggested by assimilation when fissions spectra are set to JEFF-3.1.1 evaluations. Only trends superior to posterior uncertainties were considered.

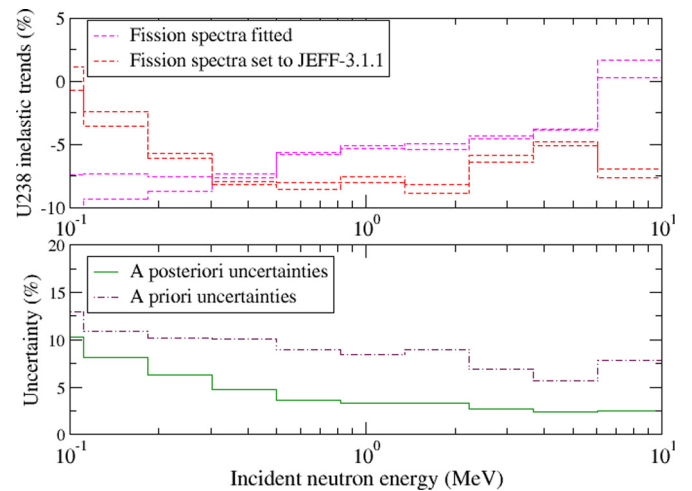
Group number	Upper energy bound	Lower energy bound	Sensitivity coefficients	Trends from assimilation (%)	Relative impact on ASTRID critical mass
4	3.68E+00	2.23E+00	-5.69E-04	-6.9	0.00004
5	2.23E+00	1.35E+00	-2.34E-03	-7.2	0.00017
6	1.35E+00	8.21E-01	-4.84E-03	-6.9	0.00033
7	8.21E-01	4.98E-01	-1.05E-02	-5.4	0.00057
8	4.98E-01	3.02E-01	-7.64E-03	-3.5	0.00027
9	3.02E-01	1.83E-01	-9.63E-03	-3.3	0.00032
10	1.83E-01	1.11E-01	-1.20E-02	-3.7	0.00045
11	1.11E-01	6.74E-02	-1.35E-02	-4.2	0.00057
12	6.74E-02	4.09E-02	-1.60E-02	-4.7	0.00076
13	4.09E-02	2.48E-02	-1.67E-02	-4.6	0.00077
14	2.48E-02	1.50E-02	-1.81E-02	-4.1	0.00074
15	1.50E-02	9.12E-03	-1.65E-02	-3.5	0.00058
Total					0.00558

**Fig. 11.** Comparison of sensitivity profiles of PROFIL-2A C/E, and FCA-IX 7 and MASURCA 1B critical masses to  $^{235}\text{U}$  and  $^{238}\text{U}$  capture.

### 3.3 $^{238}\text{U}$ inelastic cross section

As for  $^{238}\text{U}$  capture cross section, trends for  $^{238}\text{U}$  inelastic depend on whether fission spectra are fitted through assimilation or set to JEFF-3.1.1. Indeed, some of the critical configurations that are the most sensitive to  $^{238}\text{U}$  inelastic cross are also the most sensitive to  $^{238}\text{U}$  fission spectrum (FCA-IX 6, FCA-IX 7 and FLATTOP- $^{235}\text{U}$ ). Besides, all critical configurations are highly sensitive to  $^{235}\text{U}$  capture.

All sets of trends for  $^{238}\text{U}$  inelastic are shown in Figure 12, along with associated uncertainties. A posteriori uncertainties are sufficiently low in the plateau region ( $\sim 1$  to 6 MeV) to consider assimilation trends as possible recommendations. For this energy range, assimilation results propose a 4%–8% decrease (from JEFF-3.1.1  $^{238}\text{U}$

**Fig. 12.** Trends from assimilation work for  $^{238}\text{U}$  inelastic (relative to JEFF-3.1.1) compared with a priori and a posteriori nuclear data uncertainties. For both cases (fission spectra fitted or not), the two dotted lines have to be seen as an additional uncertainty associated to the choice of graphite evaluation.

inelastic cross section) depending on whether fission spectra are fitted or not. For  $^{238}\text{U}$  inelastic cross sections, differences in posterior uncertainties for these four cases do not exceed 0.5% in the energy range of interest. Thus, only one curve is displayed in Figure 12.

Assimilation results are compared to CIELO [18] (evaluation version of September the 29th, 2017), JEFF-3.1.1 and JEFF-3.3t3 [17] evaluations in Figure 13. Focusing on the plateau region, we observe that CIELO and JEFF-3.3t3 evaluations are both lower than JEFF-3.1.1 in this region, but the level of decrease is different.

Once again, the dependency of assimilation results for  $^{238}\text{U}$  inelastic cross sections on fission spectra is a hint of possible compensation errors in the results. Assimilation work can be improved with the use of a wider database including more C/Es sensitive to  $^{238}\text{U}$  inelastic cross sections.

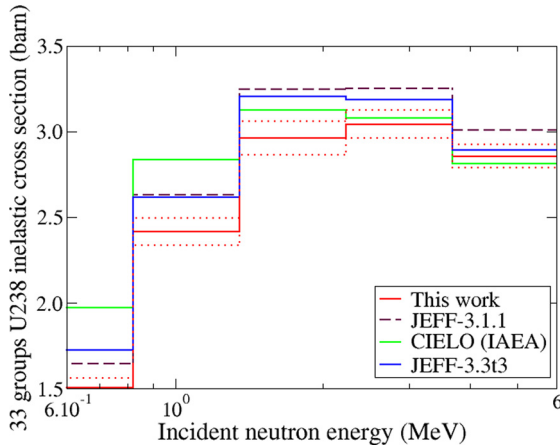


**Fig. 13.** 33-group assimilation results (case where fission spectra are not fitted and graphite evaluation used is from JEFF-3.1.1) for  $^{238}\text{U}$  inelastic compared with “a priori” JEFF-3.1.1, CIELO and JEFF-3.3t3 evaluation. Posterior uncertainties for assimilation results are in dotted line.

## 4 Conclusion

C/E values from several critical masses calculations and from PROFIL irradiation experiments were used in a Bayesian inference approach as implemented in the CONRAD code to investigate cross sections that might need reassessment. These C/E values provide a great variety of sensitivity profiles to  $^{235}\text{U}$  and  $^{238}\text{U}$  cross sections, including capture and inelastic.

Trends suggested for  $^{235}\text{U}$  capture, which are in agreement with recent differential measurements made at RPI and LANSCE, confirm that significant modifications are needed for this cross section in JEFF-3.1.1 (~30% decrease around 1–2.25 keV and ~10% increase in the 10–100 keV energy range). This issue was already addressed in WPEC Subgroup 29, which underlined an overestimation of this cross section in the end of the RRR [15]. JEFF-3.3t3 seems to go in the right direction with a decrease of around 25% from JEFF-3.1.1 in the end of RRR and an increase up to 20% in the URR. Comparisons of integral data assimilation results with recent differential measurements constitute a key step in our study as sources of uncertainties are different.

For  $^{238}\text{U}$  cross sections, results are highly dependent on whether fission spectra are fitted or not. For  $^{238}\text{U}$  capture cross section, the integral data assimilation suggests a 4%–7% decrease of the cross section from 10 keV to 3 MeV in the case where fission spectra are set to JEFF-3.1.1 evaluations. Such modifications on  $^{238}\text{U}$  capture can have a significant impact on critical mass calculations of Fast Reactors. Thus, these results should be further confirmed by assimilation results using a wider experimental database.

For  $^{238}\text{U}$  inelastic cross sections, integral data assimilation suggests a 4% to 8% decrease in the plateau region (from around 1 to 6 MeV), depending on whether fission spectra are fitted or not. JEFF-3.3t3 and CIELO evaluations also point toward a decrease from JEFF-3.1.1 in this energy region but at different levels. Previous

work from Santamarina [19], using the RDN code and targeted on integral measurements with a strong sensitivity to  $^{238}\text{U}$  inelastic cross section (including Pu-fueled systems), suggested a reduction trend of  $-11\% \pm 3\%$  (in a case where  $^{238}\text{U}$  fission spectra were not re-estimated).

In the end, this assimilation work focusing on  $^{235}\text{U}$  and  $^{238}\text{U}$  nuclear data with a reduced database enables us to deduce possible trends on these data independently from Pu isotopes nuclear data. Results presented in this work have to be confirmed by the addition of other integral experiments. Notably, trends on  $^{238}\text{U}$  capture and inelastic cross sections might possibly exhibit compensating errors. Besides, posterior uncertainties from this work are probably underestimated: indeed, we did not take into account uncertainty from nuclear data which are not fitted (structural material, fission cross sections, etc.). An attempt to take into account these approximations through marginalization is under study.

The authors express their gratitude to S. Okajima, K. Tsujimoto and M. Fukushima, from JAEA for providing detailed information on the FCA-IX experiments. The authors wish to thank J. Tommasi and E. Privas for their detailed work on the PROFIL experiments. Virginie Huy thanks EDF and CEA for their common financial support of her Ph.D.

## Author contribution statement

The results presented in this paper were produced in the framework of V. Huy PhD work. G. Rimpault and G. Noguere have contributed to this work by providing supervisory support and expert viewpoints.

## References

1. E. Brun, TRIPOLI-4, CEA, EDF and AREVA reference Monte Carlo code, in *Joint International Conference on Supercomputing in Nuclear Applications and Monte Carlo* (2015), Vol. 82, pp. 151–160
2. M. Fukushima, Y. Kitamura, T. Kugo, S. Okajima, Benchmark models for criticalities of FCA-IX assemblies with systematically changed neutron spectra, *J. Nucl. Sci. Technol.* **53**, 406 (2016)
3. C. De Saint Jean et al., Uncertainty evaluation of nuclear reaction model parameters using integral and microscopic measurements with the CONRAD code, in *ND2010 Conference* (2010)
4. T. Bayes, An essay toward solving a problem in the Doctrine of chances, *Philos. Trans. R. Soc. Lond.* **53**, 370 (1763)
5. C.E. Shannon, A mathematical theory of communication, *Bell Syst. Tech. J.* **27**, 379 (1948)
6. A. Azevedo-Filho, R.D. Shachter, Laplace’s method approximations for probabilistic inference in belief networks with continuous variables, in *Uncertainty in Artificial Intelligence Proceedings of the Tenth Conference, Seattle, Washington, USA* (1994) pp. 28–36
7. E. Privas, P. Archier, C. De Saint Jean, G. Noguère, J. Tommasi, The use of nuclear data as nuisance parameters in the integral data assimilation of the PROFIL experiments, *Nucl. Sci. Eng.* **182**, 377 (2016)

8. J. Tommasi, G. Noguere, Analysis of the PROFIL and PROFIL-2 sample irradiation experiments in Phénix for JEFF-3.1 nuclear data validation, Nucl. Sci. Eng. **160**, 232 (2008)
9. G. Rimpault, D. Plisson, J. Tommasi, R. Jacqmin, The ERANOS code and data system for fast reactor neutronic analyses, in *PHYSOR'02, Seoul, KOREA* (2002)
10. P. Archier, C. De Saint Jean, G. Noguere, O. Litaize, P. Leconte, C. Bouret, COMAC: nuclear data covariance matrices library for reactor applications, in *PHYSOR 2014–The Role of Reactor Physics Toward a Sustainable Future, Kyoto, Japan* (2014)
11. M. Herman et al., COMMARA-2.0 Neutron Cross Section Covariance Library, BNL-94830-2011, 2011
12. A.D. Carlson et al., International evaluation of neutron cross section standards, Nucl. Data Sheets **110**, 3215 (2009)
13. N. Otuka, E. Dupont, Towards a more complete and accurate Experimental Nuclear Reaction Data Library (EXFOR): International Collaboration Between Nuclear Reaction Data Centres (NRDC), Nucl. Data Sheets **120**, 272 (2014)
14. Y. Danon et al., Simultaneous measurement of  $^{235}\text{U}$  fission and capture cross sections from 0.01 eV to 3 keV using a gamma multiplicity detector, Nucl. Sci. Eng. **187**, 291 (2017)
15. O. Iwamoto, R. McKnight, International Evaluation Cooperation Volume 29: Uranium-235 Capture Cross-section in the keV to MeV Energy Region, NEA, NEA/WPEC-29, 2011
16. M. Jandel et al., New precision measurements of the  $^{235}\text{U}(n,g)$  cross section, Phys. Rev. Lett. **109**, 202506 (2012)
17. JEFF-3.3 Nuclear Data library can be downloaded on the NEA website: <https://www.oecd-nea.org/dbdata/JEFF33/>
18. M.B. Chadwick et al., The CIELO collaboration: neutron reactions on  $^1\text{H}$ ,  $^{16}\text{O}$ ,  $^{56}\text{Fe}$ ,  $^{235,238}\text{U}$ , and  $^{239}\text{Pu}$ , Nucl. Data Sheets **118**, 1 (2014)
19. A. Santamarina, Improvement of  $^{238}\text{U}$  inelastic scattering cross section for an accurate calculation of large commercial reactors, Nucl. Data Sheets **118**, 118 (2014)

**Cite this article as:** Virginie Huy, Gilles Noguère, Gérald Rimpault, Use of integral data assimilation and differential measurements as a contribution to improve  $\text{U}_{235}$  and  $\text{U}_{238}$  cross sections evaluations in the fast and epithermal energy range, EPJ Nuclear Sci. Technol. **4**, 41 (2018)